Comparing the Interaction of Platinum-Hypocrellin A Complex and Hypocrellin A with Bovine Hemoglobin

Yuan Xiuxue, Chen Enyi, Xiao Mengsi, Zhao Chuanfeng, Zhou Jiahong

(School of Chemistry and Materials Science, Analysis and Testing Centre, Jiangsu Key Laboratory of Biofunctional Materials, Jiangsu Collaborative Innovation Centre of Biomedical Functional Materials, Key Laboratory of Applied Photochemistry, Nanjing Normal University, Nanjing 210023, China)

Abstract: The interaction mechanisms of Hypocrellin A(HA) and its platinum complex(Pt-HA) with bovine hemoglobin(BHb) were compared by ultraviolet-visible(UV-Vis) absorption, time-resolved fluorescence spectra, circular dichroism(CD) and induced circular dichroism(ICD) spectra, respectively. The UV-Vis results revealed that both HA and Pt-HA could interact with BHb and the latter interaction was stronger than HA. In addition, quenching mechanism of HA and Pt-HA were both static process, which were ascribed to the electron transfer. Moreover, CD and ICD spectrum revealed that the microenvironment and conformation of BHb were changed after conjugation with HA and Pt-HA, as the latter altered more acute. Finally, the comparison results demonstrated that the interaction of Pt-HA and BHb was stronger and more stable than HA.

Key words: hypocrellin A, platinum-hypocrellin A, bovine hemoglobin, interaction

CLC number: O657.3 **Document code**: A **Article ID**: 1001-4616(2015)03-0014-11

光谱法比较光疗药物竹红菌甲素及铂竹红菌甲素复合物与牛血红蛋白的相互作用

袁秀雪,陈恩懿,肖梦思,赵传峰,周家宏

(南京师范大学化学与材料科学学院,分析测试中心,江苏省生物功能材料重点实验室,江苏省生物功能材料协同创新中心,应用光化学重点实验室,江苏 南京 210023)

[摘要] 通过紫外-可见吸收光谱、瞬态荧光光谱以及圆二色谱来比较光疗药物竹红菌甲素及铂竹红菌甲素复合物与牛血红蛋白的相互作用.结果表明,虽然竹红菌甲素及铂竹红菌甲素复合物与牛血红蛋白的反应机理都是基于电子转移的静态猝灭,但是铂竹红菌甲素复合物与牛血红蛋白的反应不仅要比竹红菌甲素强,而且反应后牛血红蛋白的微环境和构像的改变也要大于竹红菌甲素.

[关键词] 竹红菌甲素,铂竹红菌甲素复合物,牛血红蛋白,相互作用

Photodynamic therapy(PDT) was a noninvasive technique for the treatment of various cancer tumors and non-cancer diseases. It was a promising modality for the management of various tumors and nonmalignant diseases, based on the application of minimal dark toxicity photosensitizer(PS) that was selectively localized in the target tissue, activated by a specific wavelength of light and resulted in photo damage and subsequent cell death via apoptosis and/or necrosis[1,2].

As a natural PS, Hypocrellin A(HA), extracted from Hypocrella bambuase, has been receiving intensive interest according to its easy preparation and purification, high photo-toxicity but low dark-toxicity, rapid clearance

Received data: 2015-03-06.

Foundation item: Project of Department of Science and Technology of Jiangsu Province(BK20131394、BZ201210).

Corresponding author: Zhao Chuanfeng, senior engineer, majored in applied chemistry. E-mai: zhaochuanfeng@njnu.edu.cn

from normal tissues[3] and the high efficiency in generating reactive oxygen species (ROSs)[4]. Nevertheless, the poor water solubility has greatly limited its clinic application[5]. In our previous work, we have found that platinum (VI) and HA can form a complex (Pt-HA) and the complex significantly enhanced the water solubility, light stability and efficiency of $^1O_2$ generation[4], thereby exhibiting better anti-tumor activity. As a phototherapy medicine, Pt-HA was delivered into the body by intravenous injection, which would interact with various proteins and created effects on the transmission process in the blood. Therefore, it was very important to study the interaction mechanisms between the Pt-HA and the protein in the blood.

In this study, Bovine hemoglobin (BHb) was selected as a model to study the interaction mechanisms of Pt-HA under physiological conditions, due to its function of a carrier of oxygen, transporter of carbon dioxide and regulator of the pH of blood directly or indirectly[6], taking HA as a control. In addition, it also played an important role in many biologically relevant processes in life science, clinical medicine and environment[7]. The results defined the delivery mechanism of the Pt-HA in the blood and have an important practical significance on the development of the application of the PDT.

1 Materials and Methods

1.1 Materials

The stock solution of HA (19.35 mM) was obtained by adding an appropriate amount of solid HA into DMSO. Bovine hemoglobin (BHb) was purchased from Sigma, and prepared in phosphate buffers (0.1 M, pH 7.0) before each experiment without further purification. Moreover, the concentration of BHb was determined by the absorption at 404 nm (ε=41 000 L·mol^{-1}·cm^{-1}). The H_2PtCl_6 was produced by Sigma, and the mother solution was 19.30 mM after dissolving by methanol. The complex of Pt-HA was prepared as our previous work by mixing 55 μL HA and 110 μL H_2PtCl_6 in double distilled water for several minutes at the room temperature with minor stirring in the dark place. Other chemicals were all analytical grade and double distilled water was used throughout. The solution was stored in cool and dark place.

1.2 Spectroscopic measurements

1.2.1 UV-Vis spectroscopy

The UV-Vis absorption data was collected from 200 nm to 600 nm on a Varian Cary 5 000 spectrophotometer in a 1.0 cm quartz cuvette. UV-Vis titrations were performed by successive addition of HA and Pt-HA complex to 3 mL BHb solution, respectively. When experiments were carried out at different temperatures (298 K, 310 K and 315 K), the solution was equilibrated in a thermostat bath.

1.2.2 Time-resolved fluorescence spectra

The fluorescence lifetime was performed on a Horiba Jobin Yvon Fluoro Max-4 time correlation single photon counting (TCSPC) system, using a 265 nm diode laser excitation source (IBH, Nano LED, pulse Fwhm ~ 3 μs). The time resolution was estimated at 1.5 ns and repetition rate up to 1 MHz. The time ranges were 0.219 ns / channel, in 4 096 effective channels. Data were globally fitted to the appropriate exponential model after deconvolution of the instrument response function by an iterative deconvolution technique, using the IBH DAS6 fluorescence decay analysis software.

1.2.3 Steady-state fluorescence spectra

All the Steady-state fluorescence titrations were investigated on Perkin-Elmer LS-50B fluorescence spectrophotometer equipped with a xenon lamp light source, and 1.0 cm quartz cells were used for these measurements at the room temperature. Every titration was operated manually with gentle stirring.

1.2.4 Circular dichroism (CD) spectra

Circular Dichroism (CD) and Induced circular dichroism (ICD) spectrum were measured with an applied photophysics chriascan circular dichroism spectropolarimeter in 1.0 cm quartz cells at room temperature. Spectra

were scanned with 1 nm spectral bandwidth and 0.5 nm step resolution. Finally, the data were analyzed by CDNN programme.

1.2.5 Theory and calculation

1.2.5.1 Binding parameters of BHb and drugs

The binding constant of the BHb and drugs could be calculated according to the following equation[8]:

$$A_0/A - A_0 = (\varepsilon_{\mathrm{BHb}}/\varepsilon_{\mathrm{BHb\text{-}Drug}} - \varepsilon_{\mathrm{Drug}})(1 + 1/K_b[\mathrm{drug}]) , \quad (1)$$

where A_0 and A were the absorbance of BHb in the absence and presence of drug, respectively. K_b was the binding constant, $\varepsilon_{\mathrm{BHb}}$, $\varepsilon_{\mathrm{Drug}}$, $\varepsilon_{\mathrm{BHb-Drug}}$ were the absorption coefficients of BHb, Drug and the BHb-Drug adduct, respectively.

1.2.5.2 Thermodynamic parameters of the binding forces

The thermodynamic parameters, enthalpy change (ΔH), entropy change (ΔS) and free energy change (ΔG) could be calculated according to Eq.(2) and Eq.(3)[9,10], as the reaction enthalpy change was regarded as a constant even if the temperature changed little.

$$\ln K_1/K_2 = (1/T_1 - 1/T_2)\Delta H/R , \quad (2)$$

$$\Delta G = \Delta H - T\Delta S = -\mathrm{R}T \ln K_b , \quad (3)$$

where K_1 and K_2 were the combination constant of composite compound of BHb and the drug at different temperatures.

1.2.5.3 Average fluorescence lifetime

The average fluorescence lifetime could be calculated according to the following equations[11,12]:

$$f_i = B_i\tau_i / \sum_{i=1}^{3} B_i\tau_i , \quad (4)$$

$$I(t) = \sum_{i=1}^{3} f_i \exp(-t/\tau_i) , \quad (5)$$

$$\langle\tau\rangle = \sum_{i=1}^{3} f_i\tau_i , \quad (6)$$

where B was the relative contributions, τ was the lifetimes of the different components to the total decay, f_i was the pre-exponential factor and $f_1+f_2+f_3= 1$.

2 Results and Discussion

2.1 The UV-Vis absorption analysis

Both UV-Vis and fluorescence spectra were the effective techniques to explore the drug effects on protein. Moreover, the intrinsic fluorescence of BHb primarily originated from its amino acid residues[13]. However, the UV-Vis spectroscopy of BHb can present both the amino acid residues, and the heme signal, simultaneously. Thus, here, UV-Vis absorption measurement was selected to study the interaction of BHb and drugs[14,15], especially to observe the effects of drugs on heme group of BHb, directly. Hence, absorption spectra of BHb in presence and absence of drugs were recorded as shown in Fig.1. From Fig.1, we could clearly observe that BHb has three absorption bands, which were located at 274 nm (the phenyl group of tryptophan and tyrosine residues), 300 nm (ε band), and 404 nm (heme or Soret band)[6] in phosphate buffers solution. Upon gradually addition of HA and Pt-HA into BHb, the absorbance intensity at 274 nm and 300 nm were both increased while the peak at 404 nm decreased in the UV-Vis spectrum, which might conclude that both HA and Pt-HA could interact with tryptophan, tyrosine residues and heme group, which resulted in disturbing the chemical environment surrounding BHb. Moreover, the disappeared band of 274 nm of BHb in the presence of Pt-HA implied that Pt-HA interacted stronger with the tryptophan and tyrosine residues of BHb and the peptide strands of BHb molecules extended more and the hydrophobicity was decreased[16]. In addition, the absorption maximum of heme group was decreased significantly after Pt-HA treatment compared to HA, while the maximum absorption wavelengths remain unchanged. Finally, the effects of HA and Pt-HA on heme group of BHb were compared detail by calculat-

ing the absorbance intensity at 404 nm at different temperatures in Fig.2. The results suggested that the interaction of BHb with Pt-HA was stronger than HA.

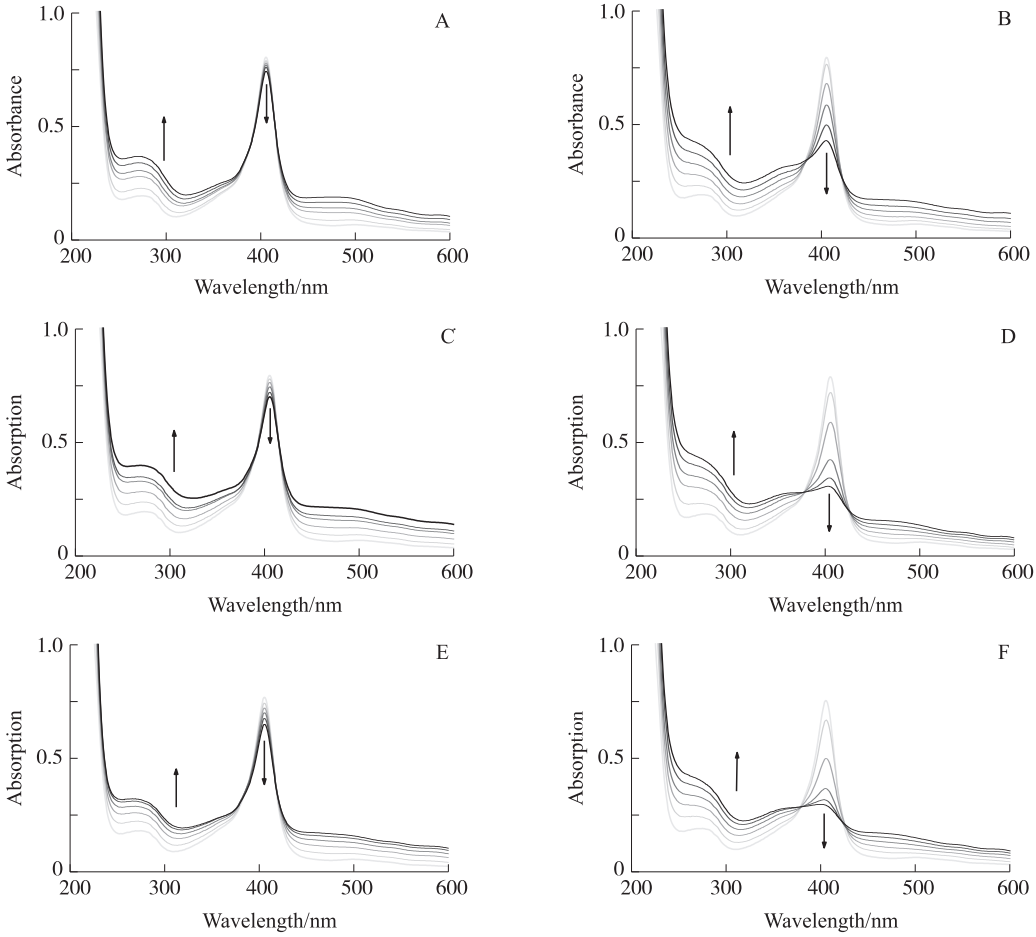

Fig.1 UV-Vis absorption spectra of pure BHb of HA(A-298 K;C-310 K;E-315 K)and UV-Vis absorption spectra of pure BHb of Pt-HA(B-298 K;D-310 K;F-315 K);[BHb]=19.9 μmol/L;[HA]=0,3.36,6.71,10.1,13.4,16.8 μmol/L;[Pt-HA]=0,3.36,6.71,10.1,13.4,16.8 μmol/L;pH=7.0

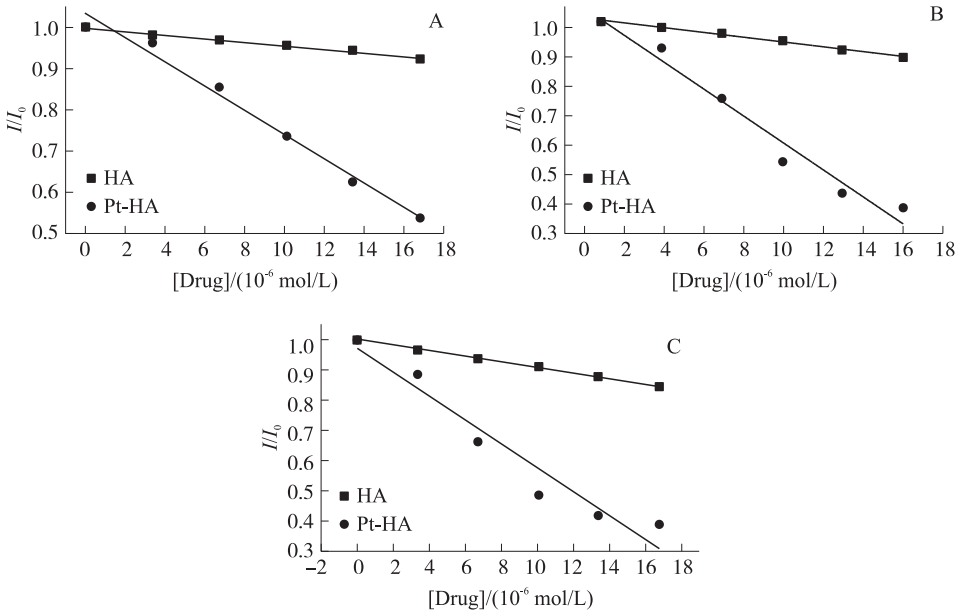

Fig.2 Plots of I/I_0 against HA and Pt-HA with different concentrations at 404 nm;[HA]=0,3.36,6.71,10.1,13.4,16.8 μmol/L;[Pt-HA]=0,3.36,6.71,10.1,13.4,16.8 μmol/L;pH=7.0,T=298 K(A),T=310 K(B),T=315 K(C).

2.2 Binding parameters of interaction

UV-Vis absorption spectroscopy was a simple but powerful way to exhibit the formation of complex when drug molecules binding with protein[17, 18]. The absorption spectrum of BHb upon continuous adding drugs at 298 K, 310 K and 315 K were exhibited in Fig.1. According to Eq.(1), the linear curve of $A_0/(A-A_0)$ vs/[Drug] were plotted as shown in Fig.3, while the K_b of HA and Pt-HA with BHb at 298 K, 310 K and 315 K were presented in Table 1, respectively. The results definitely indicated that the K_b of Pt-HA with BHb were bigger than HA with BHb, which concluded that the interaction of Pt-HA and BHb was more stable than HA.

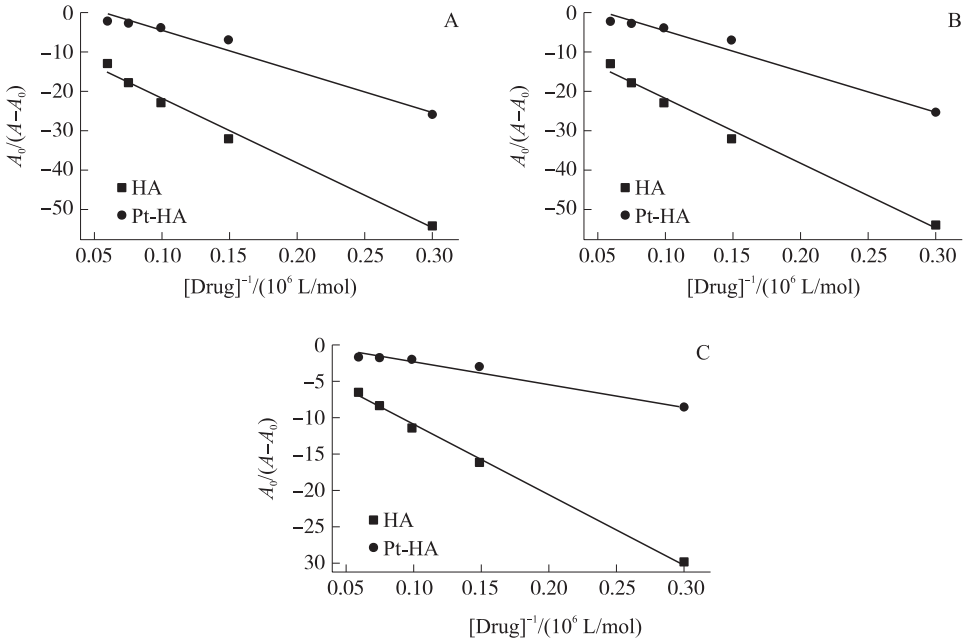

Fig.3 Plots of $A_0/A-A_0$ vs/[Drug] at different temperature 298 K(A), 310 K(B) and 315 K(C).

Table 1 Estimated values of binding constant of HA with BHb as well as Pt-HA with BHb at different temperature

Samples	Temperature (K)	$K_b/(10^4$ mol/L$)^{-1}$)
HA	298	3.33
	310	1.43
	315	1.36
Pt-HA	298	5.58
	310	3.76
	315	2.58

2.3 Thermodynamics parameters

Binding force of drug molecules to protein could be calculated by the obtained thermodynamic parameters such as enthalpy change(ΔH), entropy change(ΔS) and free energy change(ΔG) of the reaction[19]. According to the previous work[20,21], there were several acting forces between small molecular and biomacromolecule, such as hydrophobic force, hydrogen bond, van der Waals, electrostatic force and so on. When $\Delta H<0$ or $\Delta H\approx0$, $\Delta S>0$, the mainly acting force was electrostatic force; when $\Delta H<0$, $\Delta S<0$, the mainly acting force was van der Waals or hydrogen bond and when $\Delta H>0$, $\Delta S>0$, the mainly force was hydrophobic[22,23]. Considering that ΔH did not vary significantly over the working temperature range, the thermodynamic parameters could be calculated by Eq.(2) and Eq.(3), and the values were listed in Table 2, respectively. On the one hand, the negative ΔG indicated that the interaction of drugs and BHb were spontaneous. On the other hand, for HA, the negative of ΔH and positive of ΔS presented that electrostatic and hydrophobic interaction played major role[24] while the negative of ΔH and ΔS indicated that van der Waals and hydrogen bond were the mainly force for Pt-HA complex.

Table 2 Thermodynamic parameters of the binding reactions of the HA with BHb and Pt-HA with BHb

Drug	Temperature/K	ΔG/(KJ/mol)	ΔH/(KJ/mol)	ΔS/(J·mol^{-1}·K^{-1})
HA	298	−25.80	−8.15	53
	310	−24.66		
	315	−24.93		
	298	−27.08		
Pt-HA	310	−27.16	−61.15	−110
	315	−26.60		

2.4 The interaction mechanism analysis between BHb and drugs

To determine the BHb fluorescence quenching mechanism between BHb and drugs, the nanosecond fluorescence lifetime of BHb was measured by the TCSPC technique, by using 265 nm diode laser excitation where only tryptophan is excited[25,26]. The lifetimes of systems at 322 nm from BHb were collected and compared. The data were fitted using a reconvolution method of the instrument response function producing X^2(Chi. Sq.)fitting values of 1~1.40. In addition, as shown in Fig.4 and Table 3, the fluorescence evolution of pure BHb can be nicely fitted by a triple-exponential function, which contributed to three different tryptophan-heme orientations in BHb[27] and indicated three decay components. According to Eq.(4), Eq.(5)and Eq.(6), the average lifetime of pure BHb in the experimental conditions was 1.797 ns. After gradually adding HA, the shorter lifetime decreased from 1.811 ns to 1.525 ns, and the proportion of the shorter component didn't show obvious changing. The lifetime of another short component (0.356 ns) decreased to 0.294 ns and the proportion of the shorter component increased from 50.2% to 50.5%. The relative longer lifetime decreased from 6.023 ns to 5.561 ns, while the component didn't show obvious changing. The average lifetime of systems showed a variance from 1.797 ns to 1.782 ns as the HA concentration increased from 0 to 3.514 μmol/L. Therefore, for Pt-HA, the shorter lifetime decreased from 1.811 ns to 1.571 ns, and the proportion of the shorter component decreased from 32.8% to 32.5%. The lifetime of another short component(0.356 ns)decreased to 0.310 ns, and the proportion of the shorter component increased from 50.2% to 50.9%. The relative longer lifetime decreased from 6.023 ns to 5.545 ns, while the proportion of the component decreased from 17% to 16.6%. The average lifetime of systems showed a variance from 1.797 ns to 1.743 ns as gradually adding Pt-HA from 0 to 3.514 μM. It was noteworthy that in presence of HA and Pt-HA, no significant change in the tryptophan fluorescence decay parameters were observed(Table 3). Thus the average lifetimes (τ) computed from the decay parameters remained essentially unchanged. This indicated that the static mechanism was principally responsible for this interaction and implied that HA and Pt-HA do indeed bind to BHb and form the stable complex[28]. Moreover, the relative bigger average lifetime variance of BHb after adding Pt-HA also certificated the stronger interaction between BHb and Pt-HA compared to HA, which consistent with the UV-Vis analysis.

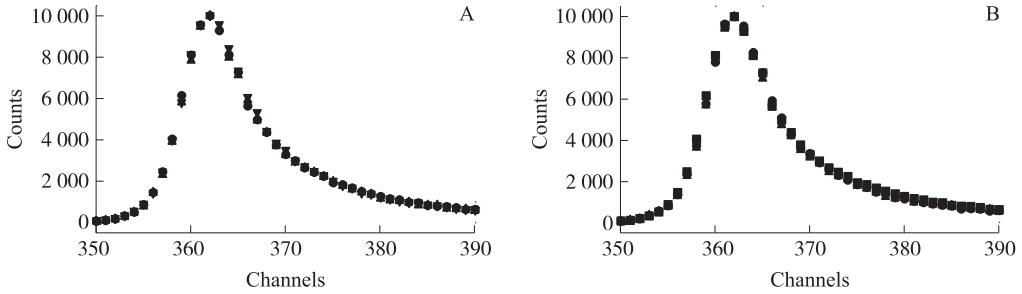

Fig.4 Time-resolved fluorescence decays for BHb in the absence and presence of HA(A)and Pt-HA(B); λ_{ex}=283 nm, [BHb]=5.0 μM; [HA]=0.000, 1.757, 3.514 μmol/L; [Pt-HA]=0.000, 1.757, 3.514 μmol/L; time calibration=2.194 787×10^{-10}s/ch.

Table 3　The fitting parameters of fluorescence lifetime of pure BHb, BHb interact with HA and Pt-HA at different concentration

Sample	C/(μmol/L)	f_1	f_2	f_3	τ_1/ns	τ_2/ns	τ_3/ns	$<\tau>$/ns
Pure BHb	5.000	0.328	0.502	0.170	1.811	0.356	6.023	1.797
BHb-HA	1.757	0.326	0.505	0.169	1.531	0.300	5.566	1.787
	3.514	0.327	0.505	0.168	1.525	0.294	5.561	1.782
BHb-Pt-HA	1.757	0.325	0.511	0.165	1.584	0.314	5.662	1.746
	3.514	0.325	0.509	0.166	1.571	0.310	5.645	1.743

To further analyze the interaction mechanism between BHb and drug, their fluorescence properties were studied. In general, BHb contained three intrinsic fluorophores (tryptophan, tyrosine, and phenylalanine residues). Besides, it has been reported that the intrinsic fluorescence of BHb primarily originated from the Trp residue alone, as the fluorescence quantum yield of phenylalanine was really very low and the tyrosine residue was mostly quenched near an amino group, a carboxyl group, or a tryptophan[29], as shown in Fig.5.

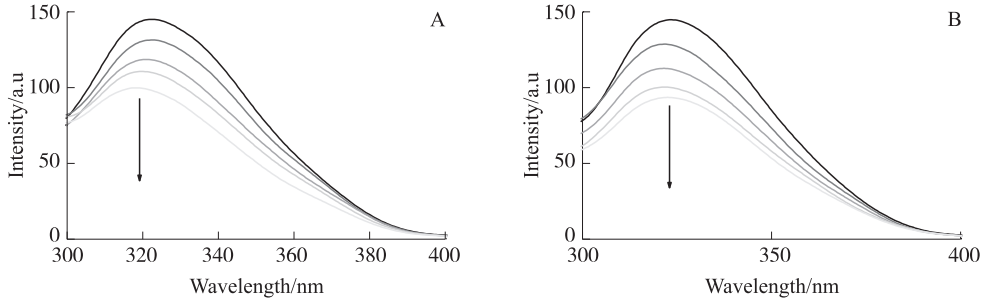

Fig.5　Fluorescence spectra of pure BHb with different HA (A) and fluorescence spectra of pure BHb with different Pt-HA (B); [BHb]=0.5 μM; [HA]=0.000, 1.757, 3.514, 5.271, 7.028, 8.758 μmol/L; [Pt-HA]=0.000, 1.757, 3.514, 5.271, 7.028, 8.758 μmol/L; λ_{ex}=285 nm, pH=7.0, T=298 K.

BHb displayed a strong fluorescence emission peaked at 322 nm after being excited with wavelengths of 285 nm in the absence of HA and Pt-HA, while HA and Pt-HA have no fluorescence signals in this experiment conditions[4]. After gradually adding HA and Pt-HA into BHb solution, the fluorescence intensity of BHb reduced gradually and blue-shifted from 322 to 318 nm, implied that there was an interaction between BHb and drug, and the changes of the microenvironment around Trp residues may contribute to the decrease of the fluorescence of BHb. In addition, in order to obtain an insight into the mechanism of fluorescence quenching, the Stern-Volmer plot, and the peak intensity as a function of the concentrations of drug, were plotted in Fig.6. It was evident that the plot showed liner behavior. In general, a linear Stern-Volmer reflected either a dynamic (collisional) or static mechanism. Dynamic quenching refer to a process that BHb and drug come into contact during the lifetime of the excited state, whereas static quenching refer to the formation of BHb-drug complex[30]. Thus, combining the results of Time-resolved fluorescence spectra, we could further conclude that the static mechanism was principally responsible for the fluorescence quenching. Moreover, the fluorescence quenching possibly could be ascribed to the energy or electron transfer from the BHb to HA or Pt-HA. Fig.7 presented the fluorescence spectrum of the drug after adding different amount BHb from 580 nm to 650 nm according to there is no fluorescence of pure BHb in this range. If HA and Pt-HA accepted the energy from BHb, the fluorescence intensity should be increased. However, it is observed that both HA and Pt-HA was quenched by BHb, which certificated the electron transfer mechanism between BHb and drug[31]. Therefore, it could be deduced that quenching mechanism of BHb and HA and Pt-HA were both static process which ascribed to electron transfer.

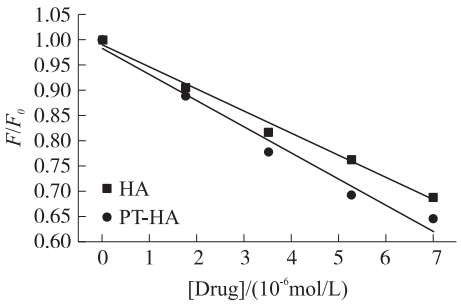

Fig.6　Plots of F/F_0 vs. [HA] and [Pt-HA] with different concentrations; [BHb]=0.5 μM; [HA]=0.000, 1.757, 3.514, 5.271, 7.028, 8.758 μmol/L; [Pt-HA]=0.000, 1.757, 3.514, 5.271, 7.028, 8.758 μmol/L; pH=7.0, T=298 K.

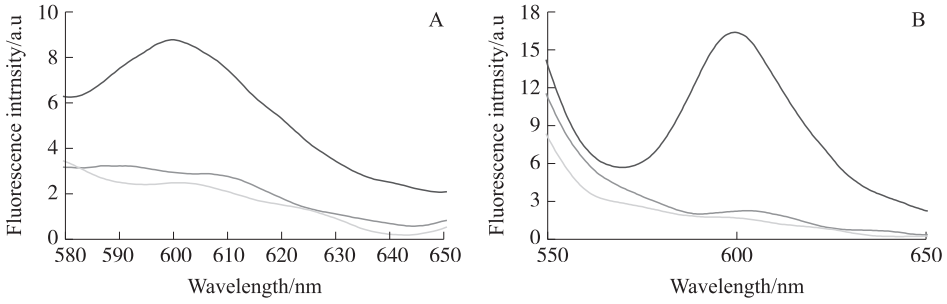

Fig.7 Fluorescence spectra of HA(A)with different BHb and fluorescence spectra of Pt-HA(B)with different BHb; [HA]=10 μmol/L;[Pt-HA]=10 μmol/L;[BHb]=0.000,1.757,3.514 μmol/L;λ_{ex}=285 nm,pH=7.0,T=298 K

2.5 Investigation on the conformation of BHb

CD spectroscopy, a sensitive technique to detect the conformation changes in protein upon interaction with drug including the changing of secondary and tertiary structures of protein[32], was employed in the following study. Fig.8 presented the CD spectra of BHb in the absence and presence HA and Pt-HA at room temperature. The CD spectrum of pure BHb showed two characteristic peaks of negative peaks at 208 nm and 222 nm, and a characteristic positive band at 215 nm[33]. The band of 208 nm was contributed to π-π* transfer for the peptide bound of α-helix, whereas the 222 nm band was contributed to π-π* transfer for both the α-helix and random coil and the 215 nm band was contributed to β-Sheet[34]. Both HA and Pt-HA have no absorption signals from 200 nm to 240 nm. After adding different amounts of HA and Pt-HA to BHb, the CD spectrum intensity of the two negative bands was decreased, whereas the positive bands rose. In addition, the CD spectrum of the BHb remains essentially unchanged upon addition of different concentrations of HA and Pt-HA(BHb concentration remaining fixed)suggested that the structure of BHb conjugate was still predominately α-helix. According to Fig.8, Pt-HA was obvious in altering indicated that the interaction between Pt-HA and BHb was stronger. In addition, through CDNN program, the secondary structural elements of pure BHb, HA-BHb, and Pt-HA-BHb were calculated and listed in the Table 4 and Table 5. Besides, they were summarized by a bar diagram in Fig.9(A)and Fig.9(B). On the basis of Table 4 and Fig.9(A), α-helix of pure BHb was 42.1% and β-sheet was 13.3%, and the amount of α-helix decreased and β-sheet increased continuously along with the continued addition of HA into BHb. Similarly, according to Table 5 and Fig.9(B), the values of α-helix decreased and β-sheet increased notably. The results suggested that both HA and Pt-HA were able to alter the secondary structure of BHb and its percentages composition of conformation, and the latter altered more acute. Moreover, the decrease of α-helix content revealed that HA and Pt-HA combined with the amino acid residues of the main polypeptide chain and further caused partial unfolding of BHb[35], the computation results presented the detail.

Induced circular dichroism (ICD) has been proved to be a sensitive technique for studies of intricate stereochemical problems related to chiral complexation and which can be applied to small organic molecules as well as large systems such as biopolymers[36]. In the range of 300 nm to 600 nm, the pure BHb has no bands. However, both HA and Pt-HA had a positive and a negative band at 355 nm and 455 nm, which were characteristic of electronic transition of n-π* of the conjugated C=O and π-π* of the large aromatic conjugated system, respectively. From Fig.10, upon gradual addition BHb into the drug, the original bands both decreased. Both the interaction indicated that drug must interact within the chiral environment of the protein, and the protein induced optical activity in the drug[37]. Besides, these changes in the ICD spectra were compared detailly as shown in Fig.11. The results implied that the BHb interacted stronger with Pt-HA at 455 nm, but slightly more acute of the interaction at 355 nm than HA due to the polymer-like structure of Pt-HA, it posses bigger aromatic conjugated system, which further certificated that the aromatic conjugated system facilitate the stronger interaction between BHb and Pt-HA.

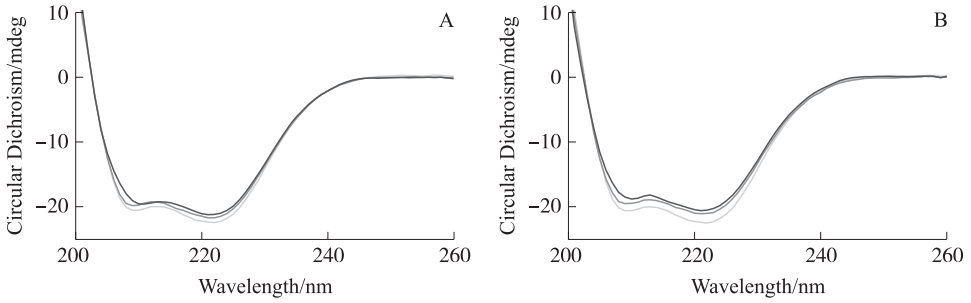

Fig.8　The CD spectra of pure BHb and HA-BHb system(A);the CD spectra of pure BHb and Pt-HA-BHb system(B)in phosphate buffers;[BHb]=0.3 μmol/L,T=298 K.

Table 4　Secondary structural elements of BHb and a function of[HA]from CD data using CDNN program

sample	C_{HA}/(μmol/L)	α-Helix/%	β-Sheet/%	β-Turn/%	Random-coil/%
BHb	0.300	42.1	13.3	15.2	28.2
BHb-HA	0.879	40.7	13.9	15.5	29.0
BHb-HA	1.757	39.4	14.3	15.6	29.9

Table 5　Secondary structural elements of BHb and a function of[Pt-HA]from CD data using CDNN program

sample	C_{Pt-HA}/(μmol/L)	α-Helix/%	β-Sheet/%	β-Turn/%	Random-coil/%
BHb	0.300	42.1	13.3	15.2	28.2
BHb-Pt-HA	0.879	39.7	14.3	15.6	29.5
BHb-Pt-HA	1.757	38.1	14.9	29.5	30.4

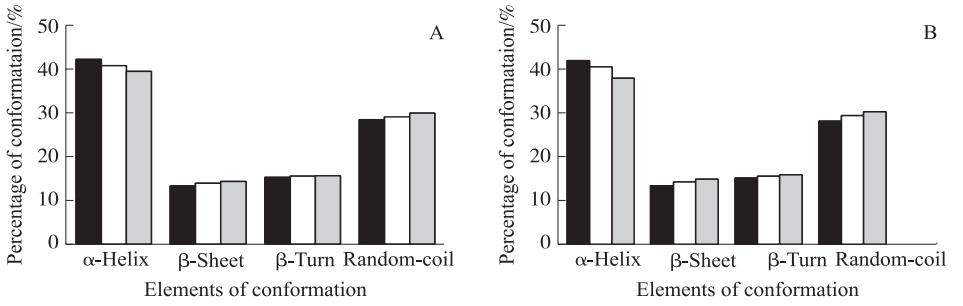

Fig.9　Bar diagrams of different conformations of BHb and HA-BHb(A)from CD data;Bar diagrams of different conformations of BHb and Pt-HA-BHb(B)from CD data;[BHb]=0.3μmol/L,[HA]=0.000(dark),0.879(white),1.757(grey)μmol/L

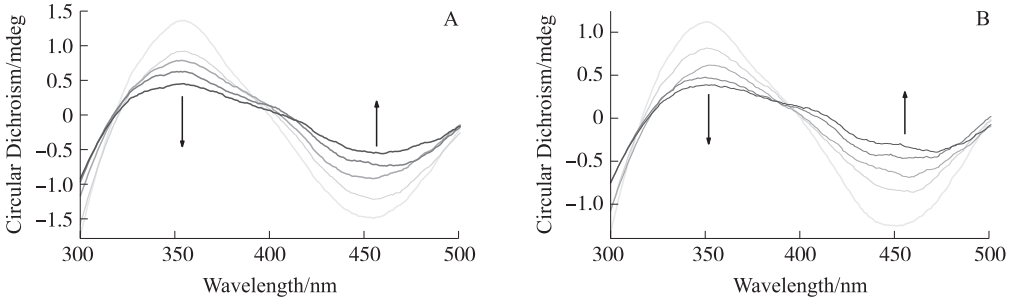

Fig.10　Induced circular dichroism(ICD)spectra of HA(A)on interaction with BHb;Induced circular dichroism(ICD)spectra of Pt-HA on interaction with BHb(B).[HA]=33.7μmol/L,[Pt-HA]=33.7μmol/L,[BHb]=0,0.043,0.086,0.129,0.172 μmol/L.

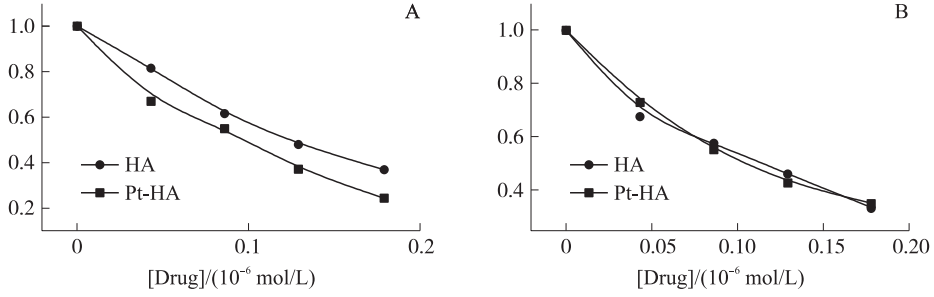

Fig.11　Comparison the interaction of drug with different amount BHb at 455 nm(A)and 355 nm(B).

3 Conclusions

The interaction of HA and Pt-HA with pure BHb were studied by employing spectroscopic techniques such as UV-Vis absorption, Time-resolved fluorescence spectra, CD and ICD spectrum. The UV-Vis spectrum indicated that both HA and Pt-HA could interact with BHb. In addition, the binding constant of Pt-HA with BHb was significant bigger than HA, and thermodynamic parameters analysis exhibited that the binding force of HA was mainly electrostatic and hydrophobic force and van der Waals and hydrogen bond force were the mainly force of Pt-HA complex. Besides, the time-resolved fluorescence and fluorescence spectrum together demonstrated that the quenching mechanism of HA and Pt-HA were static quenching due to the electron transfer from BHb to HA and Pt-HA. Finally, CD spectra provided evidences of the reducing of α-helix after interaction, supporting that the micro-environment and conformation of BHb were changed in the presence of HA or Pt-HA. The all comparison certificated the interaction of BHb with Pt-HA was more stable and stronger than HA. Finally, the results also indicated that after chelating with Pt, the prosperities of HA was improved, which would be has an important practical significance on the development of the application of the PDT.

[参考文献]

[1] Shi J J, Wang L, Gao J, et al. A fullerene-based multi-functional nanoplatform for cancer theranostic applications[J]. Biomate, 2014, 35(22): 5 771-5 784.

[2] Gorman A, Killoran J, O'Shea C, et al. In vitro demonstration of the heavy-atom effect for photodynamic therapy[J]. J Am Chem Soc, 2004, 126(34): 10 619-10 631.

[3] Yang C, Ma F, Tang J, et al. Synthesis of vanadyl-hypocrellin a complex and its photodynamic properties research[J]. Bioorg Med Chem Lett, 2012, 22(15): 5 003-5 007.

[4] Zhou L, Liu J H, Ma F, et al. Mitochondria-targeting photosensitizer-encapsulated amorphous nanocage as a bimodal reagent for drug delivery and biodiagnose in vitro[J]. Biomed Microdevices, 2010, 12(4): 655-663

[5] Ma F, Ge X F, Huang H Y, et al. Interactions of CT-DNA with hypocrellin a and its Al^{3+}-Hypocrellin A complex[J]. Spectrochim Acta Part A, 2013, 109: 158-163.

[6] Xiao M S, Han L, Zhou L, et al. Comparison and investigation of bovine hemoglobin binding to dihydroartemisinin and 9-hydroxy-dihydroartemisinin: spectroscopic characterization[J]. Spectrochim Acta Part A, 2014, 125: 120-125.

[7] Wu Y, Cui W, Zhou S, et al. The binding behavior of itraconazole with hemoglobin: studies from multi-spectroscopic techniques[J]. Spectrochim Acta Part A, 2014, 131: 407-412.

[8] Dang X J, Nie M Y, Tong J, et al. Inclusion of 10-methylphenothiazine and its electrochemically generated cation radical by β-cyclodextrin in water+ methanol solvent mixtures[J].J Electroanal Chem, 1997, 437(1): 53-59.

[9] Sun Y, Ji Z, Liang X, , et al, Studies on the binding of rhaponticin with human serum albumin by molecular spectroscopy, modeling and equilibrium dialysis[J]. Spectrochim Acta Part A, 2012, 87: 171-178.

[10] Bakkialakshmi S, Chandrakala D. A spectroscopic investigations of anticancer drugs binding to bovine serum albumin[J]. Spectrochim Acta Part A, 2012, 88: 2-9.

[11] Pradhan A, Pal P, Durocher G, et al. Steady state and time-resolved fluorescence properties of metastatic and non-metastatic malignant cells from different species[J]. J Photochem Photobiol, 1995, 31(3): 101-112.

[12] Sentchouk V V, Bodaryuk E V. Fluorescent analysis of interaction of flavonols with hemoglobin and bovine serum albumin [J]. J Appl Spectrosc, 2007, 74(5): 731-737.

[13] Wang Y Q, Zhang H M, Zhou Q H. Studies on the interaction of caffeine with bovine hemoglobin[J].Eur J Med Chem, 2009, 44(5): 2 100-2 105.

[14] Tang J, Yang C, Zhou L, et al. Studies on the binding behavior of prodigiosin with bovine hemoglobin by multi-spectroscopic techniques[J]. Spectrochim Acta Part A, 2012, 96(2 012): 461-467.

[15] Ashoka S, Seetharamappa J, Kandagal P B, et al. Investigation of the interaction between trazodone hydrochloride and bovine serum albumin[J]. J Lumin, 2006, 121(1): 179-186.

[16] Wang Y Q, Zhang H M, Zhang G C, et al. Studies of the interaction between paraquat and bovine hemoglobin[J]. Int J Biol Macromol, 2007, 41(3): 243-250.

[17] Kandagal P B, Shaikh S M T, Manjunatha D H, et al. Spectroscopic studies on the binding of bioactive phenothiazine compounds to human serum albumin[J]. J Photochem Photobiol, 2007, 189(1): 121-127.

[18] Ibrahim M S. Voltammetric studies of the interaction of nogalamycin antitumor drug with DNA[J]. Anal Chim Act, 2001, 443(1): 63-72.

[19] Xiao J, Shi J, Cao H, et al. Analysis of binding interaction between puerarin and bovine serum albumin by multi-spectroscopic method[J]. J Pharm Biomed Anal, 2007, 45(4): 609-615

[20] Gonzalez-Jimenez J, Cortijo M. Urea-induced denaturation of human serum albumin labeled with acrylodan[J]. J Protein Chem, 2002, 21(2): 75-79.

[21] Shahabadi N, Kashanian S, Darabi F. In vitro study of DNA interaction with a water-soluble dinitrogen schiff base[J]. DNA Cell Biol, 2009, 28(11): 589-596.

[22] Shahabadi N, Fatahi A. Multispectroscopic DNA-binding studies of a tris-chelate nickel(II)complex containing 4, 7-diphenyl 1, 10-phenanthroline ligands[J]. J Mol Struct, 2010, 970(1): 90-95.

[23] Guo X J, Jing K, Guo C, et al. The investigation of the interaction between oxybutynin hydrochloride and bovine serum albumin by spectroscopic methods[J]. J Lumin, 2010, 130(12): 2 281-2 287.

[24] Zhou J H, Wu X H, Gu X T, et al. Spectroscopic studies on the interaction of hypocrellin A and hemoglobin[J]. Spectrochim Acta Part A, 2009, 72(1): 151-155.

[25] Mahato M, Pal P, Kamilya T, et al. Hemoglobin-silver interaction and bioconjugate formation: a spectroscopic study[J]. J Phys Chem B, 2010, 114(20): 7 062-7 070.

[26] Yamashita S, Nishimoto E, Szabo A G, et al. Steady-state and time-resolved fluorescence studies on the ligand-induced conformational change in an active lysozyme derivative, Kyn62-Lysozyme[J]. Biochem, 1996, 35(2): 531-537.

[27] Szabo A G, Krajcarski D, Zuker M. Conformational heterogeneity in hemoglobin as determined by picosecond fluorescence decay measurements of the tryptopran residues[J]. Chem Phys Lett, 1984, 108(2): 145-149.

[28] Chaudhuri S, Chakraborty S, Sengupta P K. Probing the interactions of hemoglobin with antioxidant flavonoids via fluorescence spectroscopy and molecular modeling studies[J]. Biophys Chem, 2011, 154(1): 26-34.

[29] Baird S, Kelly S M, Price N C, et al. Hemocyanin conformational changes associated with SDS-induced phenol oxidase activation[J]. J Nairn Biochim Biophys Acta, Proteins Proteomics, 2007, 174(11): 1 380-1 394.

[30] Bi S Y, Yan L L, Wang B B, et al. Spectroscopic and voltammetric characterizations of the interaction of two local anesthetics with bovine serum albumin[J]. J Lumin, 2011, 131(5): 866-873.

[31] Yu P, Wen X M, Toh Y R, et al, Efficient electron transfer in carbon nanodot-graphene oxide nanocomposites[J]. J Mater Chem C, 2014, 2(16): 2 894-2 901.

[32] Li R, Nagai Y, Nagai M. Changes of tyrosine and tryptophan residues in human hemoglobin by oxygen binding: near-and far-UV circular dichroism of isolated chains and recombined hemoglobin[J]. J Inorg Biochem, 2000, 82(1): 93-101.

[33] Sareh S, Jamshidkhan C. Investigation on the interaction between tamoxifen and human holo-transferrin: determination of the binding mechanism by fluorescence quenching, resonance light scattering and circular dichroism methods[J]. Int J Biol Macromol, 2010, 47(4): 558-569.

[34] Bolanos-Garcia V M, Ramos S, Castillo R, et al. Monolayers of apolipoproteins at the air/water interface[J]. J Phys Chem B, 2001, 105(24): 5 757-5 765.

[35] Huang B X, Kim H Y, Dass C. Probing three-dimensional structure of bovine serum albumin by chemical cross-linking and mass spectrometry[J]. J Am Soc Mass Spectrom, 2004, 15(8): 1 237-1 247.

[36] Allenmark S. Induced circular dichroism by chiral molecular interaction[J]. Chirality, 2003, 15(5): 409-422.

[37] Mandal P, Bardhan M, Ganguly T, Spectroscopic investigations to reveal the nature of interactions between the haem protein myoglobin and the dye rhodamine 6G[J]. Lumin, 2012, 27(4): 285-291.

[责任编辑:顾晓天]